JGR Oceans

RESEARCH ARTICLE
10.1029/2021JC017386

Key Points:

- Sensitivity of meteotsunami generation and propagation to some environmental conditions is quantified in the Adriatic Sea
- Removing mountains has little impact on meteotsunamis while flattening the bathymetry diverts them from the coasts
- Extreme climate warming could increase the meteotsunami wave intensities along the most sensitive Adriatic coastal areas

Supporting Information:

Supporting Information may be found in the online version of this article.

Correspondence to:

C. Denamiel,
cdenami@irb.hr

Citation:

Denamiel, C., Tojčić, I., & Vilibić, I. (2022). Meteotsunamis in orography-free, flat bathymetry and warming climate conditions. *Journal of Geophysical Research: Oceans*, *127*, e2021JC017386. https://doi.org/10.1029/2021JC017386

Received 22 MAR 2021
Accepted 7 JAN 2022

Author Contributions:

Conceptualization: Cléa Denamiel, Ivica Vilibić
Data curation: Cléa Denamiel
Formal analysis: Cléa Denamiel, Iva Tojčić
Funding acquisition: Ivica Vilibić
Investigation: Cléa Denamiel, Ivica Vilibić
Methodology: Cléa Denamiel, Ivica Vilibić
Project Administration: Ivica Vilibić
Resources: Cléa Denamiel
Software: Cléa Denamiel
Supervision: Cléa Denamiel, Ivica Vilibić
Visualization: Cléa Denamiel
Writing – original draft: Cléa Denamiel
Writing – review & editing: Cléa Denamiel, Iva Tojčić, Ivica Vilibić

Meteotsunamis in Orography-Free, Flat Bathymetry and Warming Climate Conditions

Cléa Denamiel[1], Iva Tojčić[1,2], and Ivica Vilibić[1,2]

[1]Ruđer Bošković Institute, Division for Marine and Environmental Research, Zagreb, Croatia, [2]Institute of Oceanography and Fisheries, Split, Croatia

Abstract Due to a lack of suitable coupled atmosphere-ocean modeling tools, the atmospheric source mechanisms that trigger the potentially destructive meteotsunami waves – which occur with periods ranging from a few minutes to a few hours – have remained partially unexplored until recently. In this process-oriented numerical work we therefore investigate and quantify the impacts of orography and extreme climate changes on the generation and propagation of the atmospheric pressure disturbances that occurred during six different historical meteotsunami events in the Adriatic Sea. In addition, the impact of bathymetry, and hence Proudman resonance, on the propagation of the meteotsunami waves is investigated for the same ensemble of events. Our main findings can be summarized as follows: (a) Removing the mountains does not have a strong effect on either the generation or propagation of the meteotsunamigenic disturbances but may slightly increase their intensity, especially over land; (b) Extreme climate warming has the potential to increase the intensity of both atmospheric disturbances and meteotsunami waves near sensitive coastal areas; while (c) Flattening the bathymetry of the deepest Adriatic Sea tends to deflect the meteotsunami waves away from sensitive harbor locations. Such sensitivity studies, if generalized to other geographic locations with a higher number of events, may provide new insights into the still unknown physics of meteotsunami generation.

Plain Language Summary Among extreme sea-level hazards, meteotsunami waves – which occur at periods from a few minutes to a few hours – remain the least studied due to a lack of suitable high-resolution coupled atmosphere-ocean modeling tools. Consequently, neither the impact of orography and bathymetry on meteotsunamigenic disturbances and meteotsunami waves nor their characteristics in a projected future climate have been properly quantified. In this process-oriented numerical work we analyze these impacts using sensitivity experiments for six different meteotsunami events in the Adriatic Sea. We found that meteotsunamigenic disturbances are not strongly modulated by the orography which can reinforced their intensity, but could be significantly increased under extreme climate warming. In addition, flattening the bathymetry of the deepest ocean parts tends to deflect the meteotsunami waves away from the sensitive harbor locations. Because meteotsunami events have the potential to cause substantial human and structural damage worldwide, this type of studies may be critical to better understand their key physical processes.

1. Introduction

In recent decades, theoretical research on potentially destructive meteorological tsunami events or meteotsunamis – atmospherically-driven long-waves in the tsunami frequency band – has focused mainly on the atmospheric and resonant processes responsible for wave generation, energy transfers between atmosphere and ocean, and the influence of bathymetry on wave propagation and amplification in the ocean (Vilibić et al., 2016). At present, a solid knowledge has been built concerning the atmospheric synoptic conditions favorable to meteotsunami events (Ramis & Jansà, 1983; Vilibić & Šepić, 2017), the different types of ocean resonances (Hibiya & Kajiura, 1982; Proudman, 1929), the energy transfers (Denamiel et al., 2018; Monserrat et al., 1998), the different types of atmospheric disturbances and their propagation (Belušić et al., 2007; Horvath & Vilibić, 2014; Tanaka, 2010) and the bathymetric effects (Rabinovich, 2009; Williams et al., 2021).

Current knowledge of the physical processes driving meteotsunami events can be summarized as follows. In the atmosphere, it is known that meteotsunamigenic disturbances are atmospheric gravity waves generated by upper level jet-fronts, storms, squall lines, hurricanes, gales, etc. It is also known that these gravity waves are maintained and amplified either (a) by wave-CISK (Conditional Instability of the Second Kind) processes, through which moist processes and diabatic heating reinforce the internal waves (Lindzen, 1974; Powers, 1997)

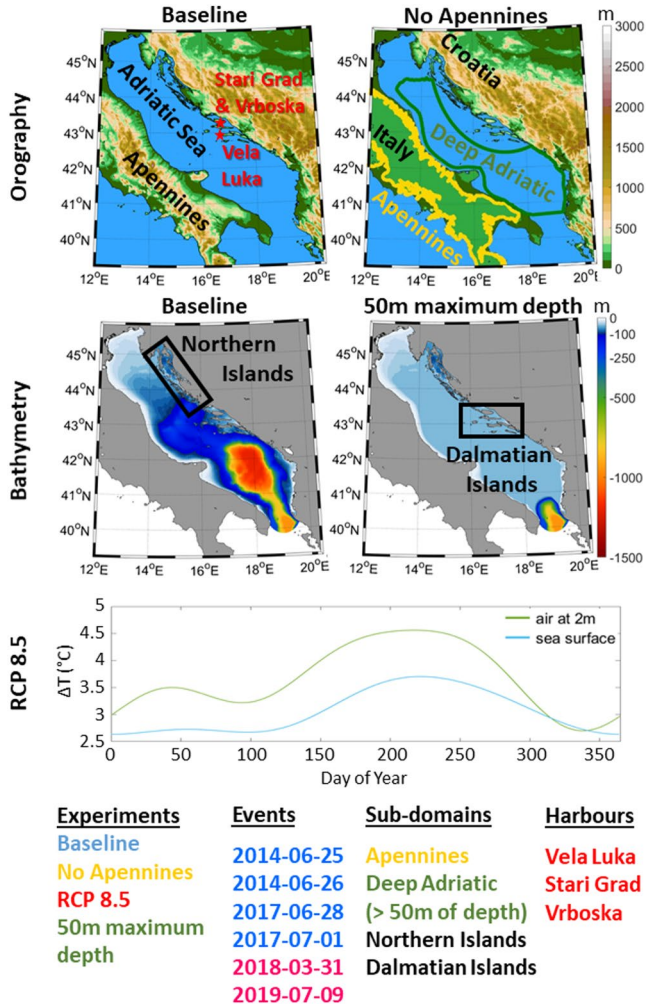

Figure 1. Experimental design of the study. Orography of the atmospheric models (top panels), bathymetry of the ocean models (middle panels) and daily climatology of the temperature changes (ΔT) under climate scenario RCP 8.5 over the atmospheric and ocean domains (bottom panel) used for the four experiments (*Baseline*, *No Apennines*, *RCP 8.5* and 50 m *maximum depth*), the six studied meteotsunami events (i.e., four *Calm Weather* events: 25 and 26 June 2014, 27 June 2017, 1 July 2017 and two *Stormy Weather* events: 31March 2018 and 9 July 2019), the four chosen sub-domains (*Apennines*, *Deep Adriatic*, *Northern Islands* and *Dalmatian Islands*) and the three sensitive harbor locations (Vela Luka, Stari Grad and Vrboska).

or (b) by wave-duct processes that occur ahead of cold fronts or gust fronts (Knupp, 2006) when a stable layer is present near the ground capped by a layer which efficiently reflects waves. In the ocean, the Proudman resonance (Proudman, 1929) is known to be the main process responsible for the energy transfer between the atmospheric gravity waves and the ocean waves and thus the meteotsunami generation (Bubalo et al., 2021; Monserrat et al., 2006; Orlić et al., 2010; Titov & Moore, 2021; Williams et al., 2021). The Proudman resonance occurs over a flat bathymetry when the speed of the atmospheric gravity waves is equal to the long-wave celerity given by $c = \sqrt{gH}$ with g the gravitational acceleration and H the ocean depth. Further, a difference of only 10% between the atmospheric disturbance and the ocean wave speeds may lower the wave height for about two times (Vilibić, 2008). In addition, the Greenspan resonance (Greenspan, 1956) is another energy transfer mechanism between the atmosphere and the ocean (e.g., Bechle & Wu, 2014; Vilibić & Šepić, 2009). It occurs on plane beaches when the speed of the atmospheric pressure disturbances in the alongshore direction is close to one of the modes of the edge wave propagation speed $c = g/\sigma\, tan[(2n + 1)\beta]$ with σ the edge wave frequency, k the wave number, n the mode number and β the slope of the beach. As for the propagation and transformation of the meteotsunami waves, they largely follow the known physics of shallow-water waves (refraction, reflection, diffraction and shoaling) and seismic waves (tsunami), as well as the known properties of standing waves when harbor resonances (or seiches) occur.

However, despite increasing scientific and computational advances, the source mechanisms and generation of the atmospheric pressure disturbances that trigger meteotsunami waves are still not fully understood. One of the major limitations faced by the meteotsunami community is that both observational networks and numerical models are generally inadequate to capture the spatially and temporarily highly variable atmospheric mesoscale structures that generate the meteotsunamigenic disturbances (Plougonven & Zhang, 2014; Rabinovich et al., 2021; Vilibić et al., 2016). Nevertheless, recent implementation of meteotsunami early warning prototypes (Anderson & Mann, 2021; Denamiel, Šepić, Huan, et al., 2019; Denamiel, Šepić, Ivanković & Vilibić, 2019; Mourre et al., 2021; Renault et al., 2011) has demonstrated that kilometer-scale atmospheric models can reproduce some pressure disturbances during meteotsunami events, although not necessarily at the correct geographic locations. Consequently, notwithstanding their potential inability to trigger an adequate response of the ocean models at sensitive locations where the events were reported, these atmospheric models can be useful tools to better understand the factors that influence the generation of meteotsunamis.

In the meteotsunami community, the Adriatic basin is historically one of the most studied areas in the world due to the 21 June 1978 event when large meteotsunami waves (6 m height for periods of about 20 min) occurred in the port of Vela Luka causing substantial damages to the infrastructures (Figure 1; Orlić et al., 2010; Vučetić et al., 2009). For this region, most of meteotsunamigenic disturbances are known to develop under similar synoptic conditions (Tojčić et al., 2021; Vilibić & Šepić, 2009) and to propagate from the Apennines to the Croatian coasts (Figure 1) with associated meteotsunami waves traveling across the Adriatic Sea (Denamiel, Huan, et al., 2020; Vilibić & Šepić, 2009). However, within the Adriatic Sea meteotsunami community, questions are still raised about (a) the influence of orography on the generation and propagation of the atmospheric disturbances, (b) their strength in the projected warmer climate, (c) the impact of offshore bathymetry on the propagation of meteotsunami waves and (d) the relative importance of the traveling meteotsunami waves generated along the Italian coasts versus the locally generated waves near

Table 1
Summary of the Adriatic Sea and Coast (AdriSC) Modeling Suite Set-Up

Module	Coupling	Domain	Model	Horizontal resolution	Region	Initial and boundary conditions (frequency)
Basic	COAWST online	Atmosphere	WRF	15 km	Middle Mediterranean Sea	ERA-Interim (6-hourly)
			WRF	3 km	Adriatic-Ionian	Two-way nesting (30 s)
		Ocean	ROMS	3 km	Adriatic-Ionian	MEDSEA (daily)
			ROMS	1 km	Wider Adriatic	One-way nesting (50 s)
Nearshore	Offline	Atmosphere	WRF	1.5 km	Adriatic Sea	WRF 3 km (hourly)
		Ocean	ADCIRC	up to 10 m	Adriatic Sea	ROMS 1 km (hourly)

the Croatian coasts. Moreover, these questions are also relevant to other meteotsunami hot-spots where they could provide critical information to assess both meteotsunami climate and coastal hazards.

To investigate these impacts, we test the sensitivity of meteotsunami generation and propagation by carrying out process-oriented numerical experiments in the Adriatic Sea (as described in Figure 1) for historical meteotsunami events previously studied with the Adriatic Sea and Coast (AdriSC) atmosphere-ocean operational model (Denamiel, Šepić, Huan, et al., 2019; Denamiel, Šepić, Ivanković & Vilibić, 2019). These experiments consist of (a) evaluating the capacity of the AdriSC model to reproduce in re-analysis mode the historical events, in both the atmosphere and the ocean, (b) testing the impact of orography on the meteotsunami genesis, in the atmosphere only, by removing the Apennines mountains, (c) assessing the impact of far future extreme climate changes on the meteotsunami generation and propagation, in both the atmosphere and the ocean, and (d) analyzing the impact of bathymetry and thus the Proudman resonance, in the ocean only, by flattening the deepest parts of the Adriatic Sea.

Hereafter, we present in detail the methods used in this study (Section 2) and examine both atmospheric pressure disturbances and resulting meteotsunami waves, obtained for the numerical simulations of the selected events, by performing three different types of analyses (Section 3). First, the regional impacts are spatially presented over the entire Adriatic domain, to identify any patterns of amplification or weakening of the meteotsunami events in both the atmosphere and the ocean. Then, the distributions of the extremes for each experiment are examined statistically for the entire set of meteotsunami events, depending on four different sub-domains important for meteotsunami generation, propagation and inundation. These statistics also consider two types of weather conditions found during meteotsunami events (Rabinovich, 2020). Finally, as meteotsunami waves are extremely sensitive to the local nearshore geomorphology, a spectral analysis is performed at known sensitive harbor locations for specific events that are well captured by the AdriSC modeling suite.

2. Methods

2.1. AdriSC Modeling Suite

The Adriatic Sea and Coast (AdriSC) modeling suite was recently implemented to simulate the atmospheric and oceanic processes driving the Adriatic basin circulation at scales ranging from long-term regional climate change to minute-by-minute impacts of extreme events along the coasts (Denamiel, Šepić, Huan, et al., 2019; Denamiel, Šepić, Ivanković & Vilibić, 2019). Due to the modular approach developed within the system, the AdriSC modeling suite can be run in both operational and research modes and has been successfully used in various applications such as climate warming research (Denamiel, Pranić, et al., 2020; Denamiel, Tojčić, Vilibić, 2020; Denamiel, Pranić, et al., 2021) or operational forecast within the Croatian Meteotsunami Early Warning System (CMeEWS; Denamiel, Šepić, Huan, et al., 2019; Denamiel, Šepić, Ivanković & Vilibić, 2019; Tojčić et al., 2021).

In this study, we use the AdriSC modeling suite with both basic and nearshore modules as described in Denamiel, Šepić, Ivanković, & Vilibić (2019) and shown in Table 1. In the basic module, the kilometer-scale regional circulation over the Adriatic-Ionian basin is derived using the Coupled Ocean-Atmosphere-Wave-Sediment Transport (COAWST) modeling system (Warner et al., 2010). Hourly results are produced at resolutions up to 3-km for the Weather Research and Forecasting (WRF) model (Skamarock et al., 2005) in the atmosphere and 1-km for the

Region Ocean Modeling System (ROMS; Shchepetkin & McWilliams, 2005, 2009) in the ocean (Table 1). In the nearshore module, the 1 min meteotsunami results presented in this article for the entire Adriatic Sea were obtained using the WRF model at 1.5-km resolution for the atmosphere (area shown in Figure 1 for orography) and, for the ocean, the 2DDI ADvanced CIRCulation (ADCIRC) model (Luettich et al., 1991) with a mesh of up to 10-m resolution in the areas sensitive to meteotsunami hazard (area shown in Figure 1 for bathymetry). Both the WRF 1.5-km and ADCIRC models are initialized and forced using the WRF 3-km and ROMS 1-km hourly COAWST results of the basic module. The impact of large-scale boundary effects within the Adriatic Sea are thus minimized.

Detailed descriptions of the AdriSC modeling suite set-up can be found in the studies by Denamiel, Šepić, Huan, et al. (2019); Denamiel, Tojčić and Vilibić (2021) and Pranić et al. (2021)

2.2. Experimental Design

2.2.1. Process-Oriented Experiments

In this study, the following process-oriented numerical experiments were performed using the AdriSC modeling suite: *Baseline*, *No Apennines*, *RCP 8.5* and *50m maximum depth*.

The *Baseline* experiment is carried out in re-analysis mode with (1) realistic orography and bathymetry (Figure 1) and (2) the COAWST model forced and initialized with the 6-hourly ERA-Interim reanalysis fields (Dee et al., 2011) in the atmosphere and the daily re-analysis MEDSEA-Ocean fields (Pinardi et al., 2003; Simoncelli et al., 2019) in the ocean.

The *No Apennines* experiment is designed to test the influence of the Apennines mountains (presenting several peaks above 2,500 m of altitude and having its highest point at 2,912 m of altitude) on the meteotsunami generation. It is similar to the *Baseline* experiment but the orography of the WRF models is modified to flatten the Apennine mountains to 150 m of altitude (Figure 1).

The *RCP 8.5* experiment follows the pseudo-global warming (PGW) methodology presented in Denamiel, Pranić, et al. (2020). It adds, to the initial and boundary conditions used in the *Baseline* experiment, three-dimensional and surface climatological changes (of air temperature, relative humidity, wind velocities, ocean temperature, salinity and ocean currents) due to the expected warming in the Representative Concentration Pathway (RCP) 8.5 scenario for the 2,070–2,100 period (e.g., climatological changes in air and sea surface temperature ΔT are shown in Figure 1 for illustrative purpose). In addition, the PGW methodology is presented in more detail in the Supporting Information S1 (Text S1).

Finally, the 50 m *maximum depth* experiment is conducted like the *Baseline* experiment but with the bathymetry of the ROMS and ADCIRC models modified to flatten the deepest part of the Adriatic Sea to 50 m of depth (Figure 1). This experiment tests the impact of the Proudman resonance (Hibiya & Kajiura, 1982; Proudman, 1929) at about 22 m/s (i.e., $C = \sqrt{gH} \approx 22$ m/s with the depth $H = 50$ m and the gravitational acceleration $g \approx 9.81$ m/s^2) on the meteotsunami wave generation and the impact of shallower depth on the meteotsunami wave propagation.

2.2.2. Studied Historical Events

Despite being regular events in the Adriatic Sea, only few well-documented historical meteotsunami events have been numerically reproduced with realistic forcing due to the lack of suitable observational networks and numerical models. In this work, we chose to study six events previously simulated in operational mode with the AdriSC modeling suite (Denamiel, Šepić, Huan, et al., 2019; Denamiel, Šepić, Ivanković & Vilibić, 2019). They occurred on 25 and 26 June 2014, 28 June 2017, 1 July 2017, 31 March 2018 and finally, 9 July 2019. It should be noted that this ensemble of events may be too small to extract fully robust statistics, but it can be used to quantify the impact of the chosen orography, bathymetry and climate changes on these specific meteotsunamis and to draw some preliminary conclusions.

These six historical meteotsunami events took place in the middle Adriatic basin and were responsible for major flooding in at least one of the three sensitive harbor locations selected in this study: Vela Luka, Stari Grad and Vrboska (Figure 1). With the exception of the 26 June 2014 event when the floods occurred in the southern Croatian towns of Rijeka dubrovačka and Ston. For example, eyewitnesses and/or tide gauge measurements reported

maximum elevations reaching up to 1.5 m on 25 June 2014 in Vela Luka, 0.75 m on 28 June 2017 in Stari Grad and 0.75 m on 25 June 2014 in Vrboska (Šepić, Međugorac, et al., 2016).

In addition, these well-documented events were previously used to evaluate the performance of both the meteotsunami forecast component of the AdriSC modeling suite (Denamiel, Šepić, Ivanković & Vilibić, 2019) and the stochastic surrogate model of the CMeEWS (Denamiel, Huan, et al., 2020; Denamiel, Šepić, Huan, et al., 2019; Tojčić et al., 2021). These evaluations performed against a set of up to 48 air-pressure sensors and 19 tide gauges revealed that, in forecast mode, (a) the WRF 1.5-km model could always reproduce some meteotsunamigenic disturbances but not necessarily their correct intensity or propagation direction, (b) the ADCIRC model could fail to capture the observed meteotsunami waves when the modeled atmospheric disturbances were even slightly shifted in location and (c) the surrogate model could systematically assess the meteotsunami hazards despite the shortcomings of the AdriSC deterministic forecasts.

For each year and experiment, the COAWST simulation starts 2 days before the first meteotsunami event of the year and runs continuously to cover all historical meteotsunami events. The WRF 1.5-km and ADCIRC simulations start 36 hr later and run till the end of the COAWST simulation. Specifically, the COAWST simulations start at 00:00:00 UTC (a) on 23 June for a duration of 4 days in 2014, (b) on 26 June for a duration of 6 days in 2017, (c) on 29 March for a duration of 3 days in 2018 and finally, (d) on 7 July for a duration of 3 days in 2019. All experiments are analyzed hereafter during the 24 hr of the meteotsunami events, this represents 24 days of 1 min atmospheric and ocean results in total.

2.3. Data Analysis

In this study we analyze the 1 min results of both mean sea-level pressure in the atmosphere (WRF 1.5-km model) and sea-level height in the ocean (ADCIRC model) over a period of 24 hr (starting at 22:00:00 UTC the day before the event) for a total of 24 events (six meteotsunami events for four experiments).

First, a Lanczos high-pass filter (Lanczos, 1956) with a 2-hr cut-off period is applied to the 1 min results of both WRF 1.5 km and ADCIRC models. The Lanczos filter is a Fourier method of filtering digital data designed to reduce the amplitude of the Gibbs oscillation. The resulting filtered air-pressure and filtered sea-level height spatial fields are presented in the Supporting Information (Movies S1–S6). The air-pressure rate of change (or pressure jump) is defined as the time derivative of the filtered mean sea-level pressure over a 4 min period (Denamiel, Šepić, Huan, et al., 2019). Throughout this work, the atmospheric disturbances are defined with the 1 min air-pressure rate of changes (i.e., pressure jumps) and the meteotsunami waves with the 1 min filtered sea-level heights.

Second, the regional changes coming from the experiments are presented as the maximum over time of air-pressure rate of change and filtered sea-level height results for each event. The spatial variations of the maximums are shown for the *Baseline* experiment while the relative changes (in percentage) is defined by the biases between the maximums of the process-oriented simulations and the *Baseline* experiment normalized by the *Baseline* experiment, and displayed for the *No Apennines*, *RCP 8.5* and 50 m *maximum depth* experiments.

Then, to perform some statistical analyses, the Adriatic basin is divided in four sub-domains (Figure 1): (a) *Apennines* which covers the area where the Apennine mountains are flatten to 150 m in the *No Apennines* experiment, (b) *Dalmatian Islands* as well as (c) *Northern Islands* which are only defined over the sea within the areas presented in Figure 1 and, finally, (d) *Deep Adriatic* which covers the sea area where the bathymetry of the Adriatic Sea is flatten to 50 m depth but excludes the parts of the domain already covered by the *Dalmatian Islands* and *Northern Islands* sub-domains. In addition, two types of meteotsunami events are distinguished following the classification by Rabinovich (2020) based on the type of atmospheric processes that trigger the meteotsunami waves. The *Calm Weather* conditions mostly refer to wave-ducting mechanism maintained in the middle troposphere (Lindzen & Tung, 1976; Monserrat & Thorpe, 1996) while the *Stormy Weather* conditions occur throughout the whole troposphere with a burst at the surface (e.g., wave-CISK, Belušić et al., 2007; squall lines, Churchill et al., 1995; frontal zones, Proudman, 1929; hurricanes, Shi et al., 2020). Hereafter, 25 and 26 June 2014, 28 June 2017 and 1 July 2017 are referred as *Calm Weather* events, with calm weather at the ground level and extremely energetic wind conditions at 500 hPa of height. The 31 March 2018 and 9 July 2019 are referred as *Stormy Weather* events with wind storms at the ground. Within the four selected sub-domains and for the four experiments, statistics for both air-pressure rate of change in the atmosphere and filtered sea-level height in the

ocean are presented as (a) violin plots (Hintze & Nelson, 1998) of the distributions of the 98th percentile calculated for the entire duration of the events at each point of the sub-domain, depending on the two event sub-categories (in the Supporting Information S1, Text S2) and (b) time variations of the 98th percentile calculated every minute for all points of the sub-domain, depending on the six studied events.

Finally, as the amplification of the meteotsunami waves highly depends on the local geomorphology of the sensitive locations, a spectral analysis is performed for the 1 min filtered mean sea-level height results in Stari Grad for the 25 June 2014 event, in Vela Luka for the 28 June 2017 and in Vrboska for the 9 July 2019. For this analysis, the wavelet power spectra in the time-period domain illustrate the temporal change of the variance contained at different periods for the *Baseline* experiment. Similarly, the wavelet coherences in the period-time domain show how the *No Apennines*, *RCP 8.5* and 50 m *maximum depth* experiments are correlated to the *Baseline* experiment. The presented results for these spectra are nearly all in the period-time domain at which the variability of the signal is significant (i.e., within the 95% confidence level against red noise represented with black lines). We used the Matlab toolbox by Grinsted et al. (2010) to compute and plot normalized Morlet wavelet power spectra and wavelet coherences for the continuous wavelet transform.

Additionally, it is important to note that, as the atmospheric *Baseline* experiment fields are not changed for the 50 m *maximum depth* experiment, only the results of the filtered sea-level height are presented for this experiment. Similarly, as the *Apennines* sub-domain is entirely located over the land, only the air-pressure jump results are presented for this sub-domain.

3. Results

3.1. Modeled Meteotsunami Events

In the presented sensitivity analysis, our aim is not to perfectly reproduce the six historical meteotsunami events chosen in this study but to compare the impact of orography, bathymetry and climate change on the atmospheric disturbances and the resulting meteotsunami waves. In order to visually qualify the capacity of the AdriSC model to simulate these impacts, the 5 min evolution of the filtered mean sea-level pressures (i.e., proxy for the atmospheric disturbances) and associated filtered sea-level height (i.e., proxy for the meteotsunami waves) for the *Baseline*, *No Apennines*, *RCP 8.5* and *50m maximum depth* experiments are presented as supporting information with one mp4 video per event (Movies S1–S6). These videos reveal that, while the 25 June 2014, 26 June 2014 and 9 July 2019 events are likely to be well reproduced, the modeled atmospheric disturbances of the 28 June 2017 event are too south to affect the Stari Grad harbor which was actually flooded, and are instead likely to trigger meteotsunami waves in the Vela Luka harbor. Finally, for both the 1 July 2017 and 31 March 2018 events, the intensities of the reproduced meteotsunami waves are far too low to properly generate any flooding. However, these events may still be used to quantify the impact of the climate change and the Apennines removal on the atmospheric disturbances and are retained in the analyses.

3.2. Regional Analysis

As a first assessment of the sensitivity of the meteotsunami genesis and propagation, the relative changes (in percentage) of the *No Apennines*, *RCP 8.5* and, for the ocean only, *50m maximum depth* experiments are regionally compared to the *Baseline* experiment for each modeled event. Hereafter, the comparison is made for the maxima in time of both air-pressure rates of change (Figures 2 and 3) and filtered sea-level heights (Figures 4 and 5).

For the 25 June 2014 event, the *Baseline* experiment shows the presence of strong atmospheric disturbances (up to 1.2 hPa/min) that trigger intense meteotsunami waves (more than 0.10 m) in the middle Adriatic Sea and along the coasts of the *Dalmatian Islands* sub-domain as well as mild atmospheric disturbances in the northern Adriatic Sea. The removal of the Apennine mountains (the *No Apennines* experiment) tends to strongly increase the northern Adriatic atmospheric disturbances (above 150%) and the meteotsunami waves along the coasts of the *Northern Islands* sub-domain (about 100%). It also increases by about 75% the meteotsunamigenic disturbances and about 60% the meteotsunami waves in the middle Adriatic. Under climate warming (the *RCP 8.5* experiment), the baseline atmospheric disturbances decrease by up to 75% and shift northward with an increase by more than 150% of the maximum pressure jumps. Consequently, the maximum filtered sea-level heights are decreased by nearly 100% along the maxima of the *Baseline* meteotsunami waves but increased by more than 100% along

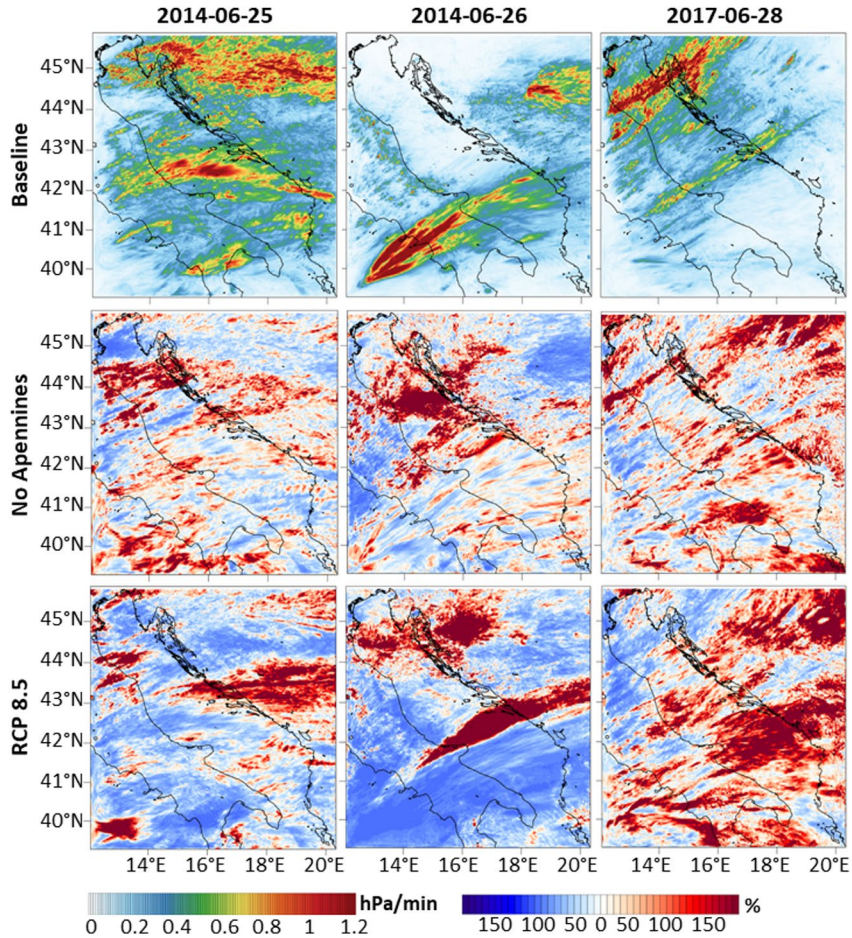

Figure 2. Regional imprint of the sensitivity experiments on the atmospheric pressure disturbances (Part 1). *Baseline* maximum air-pressure rates of change (top panels) as well as *No Apennines* (middle panels) and *RCP 8.5* (bottom panels) relative changes (in percentage) for the maximum air-pressure rate of change during the 25 and 26 June 2014, and 28 June 2017 events.

the northern coastline of the *Dalmatian Islands* sub-domain. Finally, the impact of the *50m maximum depth* experiment on the meteotsunami waves is mostly to decrease their intensity by up to 70% along the path of the *Baseline* maxima and to divert them toward the southern Adriatic Sea where their intensity is increased by more than 100%.

For the 26 June 2014 event, strong *Baseline* pressure jumps (more than 1.2 hPa/min) are located in the southern Adriatic Sea and drive traveling meteotsunami waves of about 0.07 m of height, which amplify up to 0.10 m along the south-eastern coasts. As previously, the *No Apennines* experiment is largely increasing the atmospheric disturbances (more than 150%) and the meteotsunami waves (up to 100%) in the northern Adriatic Sea, but mildly changes them (±70% in the atmosphere and ±50% in the ocean) along the meteotsunamigenic banners reproduced for the *Baseline* experiment. The changes for the *RCP 8.5* experiment are stronger, with a northward shift of the meteotsunamigenic disturbances revealing an increase of more than 150% and 100% in the air-pressure rates of change and the filtered mean sea-level heights, respectively. Southward, a decrease of these conditions (up to 100% in the atmosphere and 75% in the ocean) occurs. Finally, as previously, the *50m maximum depth* experiment diverts the meteotsunami waves southward (increase of more than 100% of the heights) but also, more surprisingly, northward with up to a 75% increase along the path of the *Baseline* disturbances.

For the 28 June 2017 event, the *Baseline* atmospheric disturbances occur at two locations: (a) the middle Adriatic with maximum pressure rates of change of about 0.7 hPa/min associated with meteotsunami waves of 0.04 m height and up to 0.1 m along the coasts of the *Dalmatian Islands* sub-domain, as well as (b) the northern Adriatic

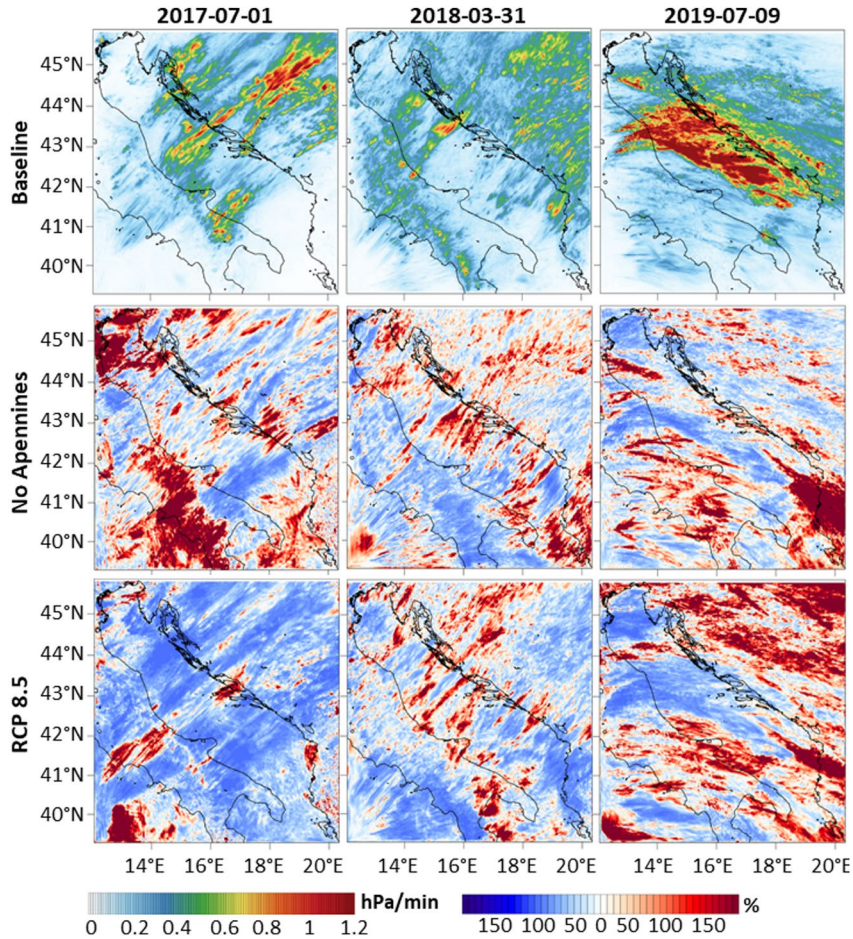

Figure 3. Regional imprint of the sensitivity experiments on the atmospheric pressure disturbances (Part 2). *Baseline* maximum air-pressure rates of change (top panels) as well as *No Apennines* (middle panels) and *RCP 8.5* (bottom panels) relative changes (in percentage) for the maximum air-pressure rate of change during the 1 July 2017, 31 March 2018 and 9 July 2019 events.

with maximum pressure jumps above 1.2 hPa/min and meteotsunami waves up to 0.10 m within the *Northern Islands* sub-domain. Both maximum pressure jump and sea-level height increase up to 150% and 100%, respectively, for the *No Apennines* experiment, while, for the *RCP 8.5* experiment, decreasing up to 100% in the northern Adriatic Sea and increasing by more than 100% in the middle and southern Adriatic Sea. As for the 2014 events, the *50m maximum depth* experiment diverts the meteotsunami waves toward the southern Adriatic (more than 100% increase of the maximum height), but also northward from the *Baseline* maximum with a filtered sea-level height increase of about 75%.

For the 1 July 2017 event, the strongest *Baseline* pressure jumps (up to 1.0 hPa/min) take place northward and southward of the *Dalmatian Islands* sub-domain, in areas where they don't have the potential to generate strong meteotsunami waves in the ocean (maximum filtered sea-level heights below 0.03 m). For the *No Apennines* experiment, the maximum air-pressure rates of change substantially increase (more than 150%) over the Apennine mountains and along the nearshore areas of the *Dalmatian Islands* sub-domain, and decrease by 100% along the southern path of the *Baseline* experiment. Consequently, the meteotsunami waves also increase in the middle Adriatic (more than 100%) but decreased (up to 100%) in the southern Adriatic.

The *RCP 8.5* experiment reveals an increase of the atmospheric disturbances (more than 150%) and the meteotsunami waves (more than 100%) in the middle Adriatic and along the *Dalmatian Islands* sub-domain, but a decrease by up to 100% everywhere else. As before, the *50m maximum depth* experiment diverts the meteotsunami waves

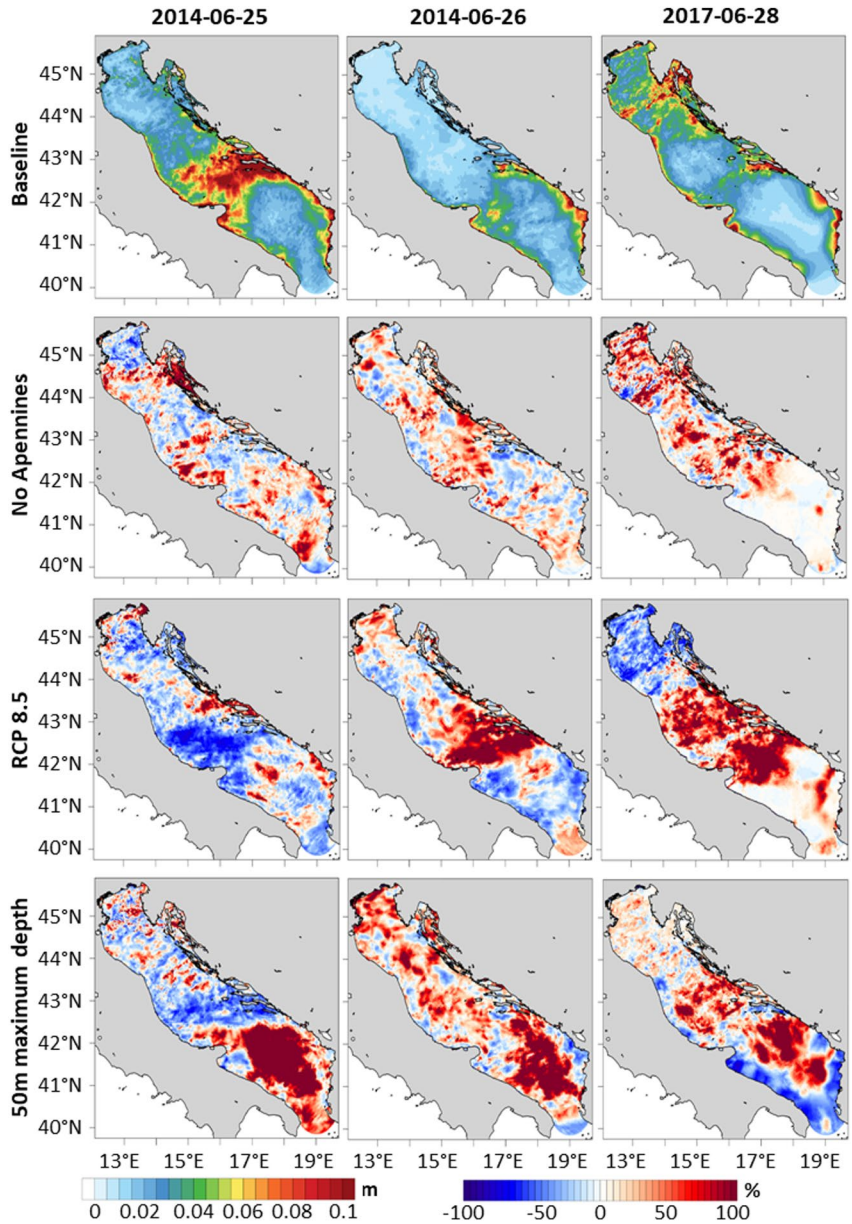

Figure 4. Regional imprint of the sensitivity experiments on the meteotsunami waves (Part 1). *Baseline* maximum filtered sea-level height (top panels) as well as *No Apennines* (middle panels), *RCP 8.5* (middle panels) and *50m maximum depth* (bottom panels) relative changes (in percentage) for the maximum filtered sea-level height during the 25 and 26 June 2014, and 28 of June 2017 events.

northward and southward from the path of the Baseline experiment, with up to 100% maximum height increase over these areas.

For the 31 March 2018 event, the strongest *Baseline* atmospheric disturbances (up to 1.0 hPa/min) are located north of the *Dalmatian Islands* sub-domain and generate moderate meteotsunami waves (up to 0.07 m) mostly along the coasts of the *Northern Islands* sub-domain. An increase of more than 150% of the pressure jumps as well as between 70% and 100% of the filtered sea-level heights is produced by both *No Apennines* and *RCP 8.5* experiments along the original path of the *Baseline* conditions but also in the nearshore areas of the *Dalmatian Islands* sub-domain. Not surprisingly, the *50m maximum depth* meteotsunami waves are again diverted southward and northward of the path of the *Baseline* waves, with more than 100% maximum height increase over these areas.

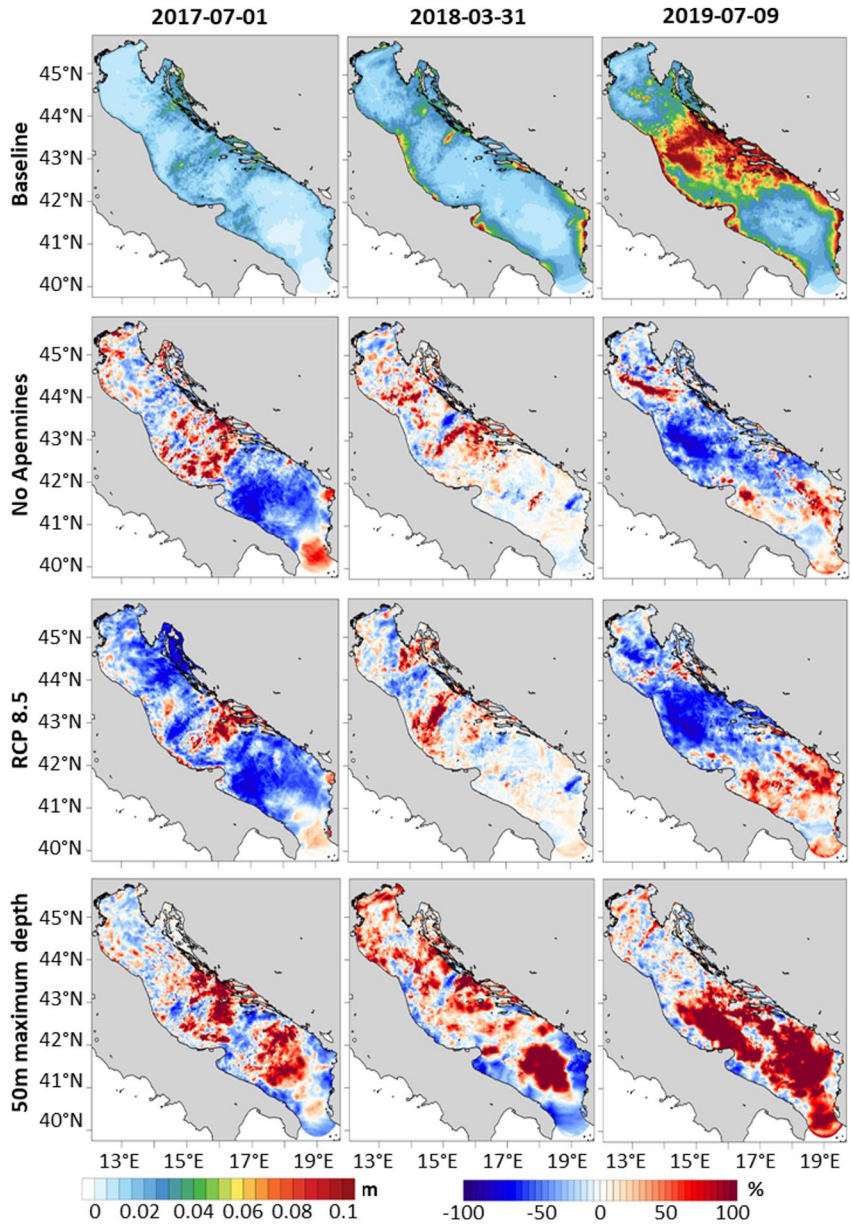

Figure 5. Regional imprint of the sensitivity experiments on the meteotsunami waves (Part 2). *Baseline* maximum filtered sea-level height (top panels) as well as *No Apennines* (middle panels), *RCP 8.5* (middle panels) and *50m maximum depth* (bottom panels) relative changes (in percentage) for the maximum filtered sea-level height during the 1 July 2017, 31 March 2018 and 9 July 2019 events.

For the final studied event, the 9 July 2019, the direction of propagation of the *Baseline* meteotsunamigenic conditions is north-west to south-east, contrarily to the other events that are aligned in direction of meteotsunamigenic banners from south-west to north-east directions. During this storm, the atmospheric disturbances are extremely intense (above 1.2 hPa/min) along the entire coastline of the middle Adriatic basin between 41°N and 44°N of latitude. Consequently, the *Baseline* meteotsunami waves are also extremely strong (above 0.10 m) in this same area. Here, both *No Apennines* and *RCP 8.5* experiments largely decrease the intensity of the *Baseline* experiment (up to 100% in the atmosphere and the ocean) in the open sea and within the nearshore areas of the *Dalmatian Islands* sub-domain for the *RCP 8.5* experiment. However, they both increase the meteotsunami conditions by up to 100% in the southern Adriatic Sea. Additionally, the *50m maximum depth* meteotsunami waves increase more than 100% over the entire Adriatic Sea below 43°N of latitude.

From this regional analysis, we can't draw general conclusions concerning the impacts on meteotsunami conditions of the Apennine mountain removal (the *No Apennines* experiment) or of the extreme climate warming (the *RCP 8.5* experiment) as they seem to vary from event-to-event. Nevertheless, we can conclude that the flattening of the bathymetry (the *50m maximum depth* experiment) always divert the meteotsunami waves from the coasts of the *Dalmatian Islands* sub-domain, where the most destructive meteotsunami events are known to occur.

3.3. Statistical Analysis

In order to better quantify the impact of the different experiments, statistical analyses are performed on four separated sub-domains (*Apennines*, *Deep Adriatic*, *Northern Islands* and *Dalmatian Islands*) for the air-pressure rate of change (i.e., pressure jump) and filtered sea-level height extremes defined as the 98th percentile: (a) in time for all points and two weather type sub-categories (*Calm Weather* and *Stormy Weather*) of events presented as violin plots (Text S2 and Figure S1 in the Supporting Information S1), and (b) in space for all times presented as 1 min time series for each event (Figure 6, analyzed hereafter).

For the *Apennines* sub-domain, in the atmosphere, the *RCP 8.5* pressure jumps are mostly weaker than for the *Baseline* and *No Apennines* experiments for the entire duration of the *Calm Weather* events, while the *No Apennines* rate of change peak values (up to 0.35 hPa/min) tend to surpass their *Baseline* counterparts. However, the peaks of the *Stormy Weather* events are higher for the *Baseline* experiment (up to 0.20 hPa/min) than for the *No Apennines* and *RCP 8.5* experiments (below 0.15 hPa/min). This is not necessarily in contradiction with the violin plot distributions (Supporting Information S1) showing an increase of extremes over the entire domain for the *RCP 8.5* experiment, as the 98th percentiles over the entire domain and events can be higher than the 98th percentiles for each time of the event.

For the *Deep Adriatic* sub-domain, in the atmosphere, the *Baseline* pressure jump peaks (up to 0.35 hPa/min) increase (1) for the *No Apennines* experiment (up to 0.50 hPa/min) for the 25 June 2014, 28 June 2017 and 31 March 2018 events and (2) for the *RCP 8.5* experiment (up to 0.40 hPa/min) for the 26 June 2014 event. In the ocean, the *RCP 8.5* filtered sea-level heights generally increase with respect to the *Baseline* values for the 28 June 2017, 31 March 2018 and 9 July 2019 events. For the 25 and 26 June events, the *Baseline* filtered sea-level heights decrease under the *RCP 8.5* scenario, but slightly increase under the *No Apennines* and *50m maximum depth* experiments.

For the *Northern Islands* sub-domain, in the atmosphere, the *No Apennines* air-pressure rates of change are consistently higher or similar to the *Baseline* values (e.g., reaching the respective values of 1.00 hPa/min and 0.60 hPa/min during the 28 June 2017). Further, the *RCP 8.5* pressure jumps are always less energetic than the *Baseline* values, except for the 28 June 2017 when the first peak of the event reaches nearly 0.60 hPa/min instead of 0.30 hPa/min. In the ocean, the peaks of the *No Apennines* and 50 m *maximum depth* filtered sea-level heights are most of the time higher or similar to the *Baseline* respective values and, for the 28 June 2017 event, the *RCP 8.5* scenario is characterized by the strongest peak of all *Calm Weather* events, reaching up to 0.135 m.

Finally, within the *Dalmatian Islands* sub-domain, in the atmosphere, the pressure jump peaks for the *RCP 8.5* experiment largely surpass the ones for the *Baseline* and *No Apennines* experiments for the 25 June 2014 (0.70 hPa/min instead of 0.55 hPa/min), 26 June 2014 (1.10 hPa/min instead of less than 0.10 hPa/min) and 28 June 2017 (0.65 hPa/min instead of respectively 0.40 and 0.50 hPa/min) events. For these events, the atmospheric disturbances generate strong meteotsunami waves with values above 0.150 m: Up to 0.250 m for the 25 June 2014, and up to 0.300 m for the 26 June 2014 and the 28 June 2017. For all the events, the *50m maximum depth* filtered sea-level heights tend to largely decrease, with values below 0.100 m, except during the last hours of the 9 July 2019 event. Further, the *No Apennines* filtered sea-level heights also seem to slightly decrease for all the events.

From these statistical analyses, we thus demonstrate that the atmospheric disturbances increase during the *Calm Weather* events for (a) the *No Apennines* experiment within the *Apennines* sub-domain with no notable change concerning the meteotsunami waves and (b) for the *RCP 8.5* experiment within the *Dalmatian Islands* sub-domain with a clear increase of the meteotsunami wave intensities.

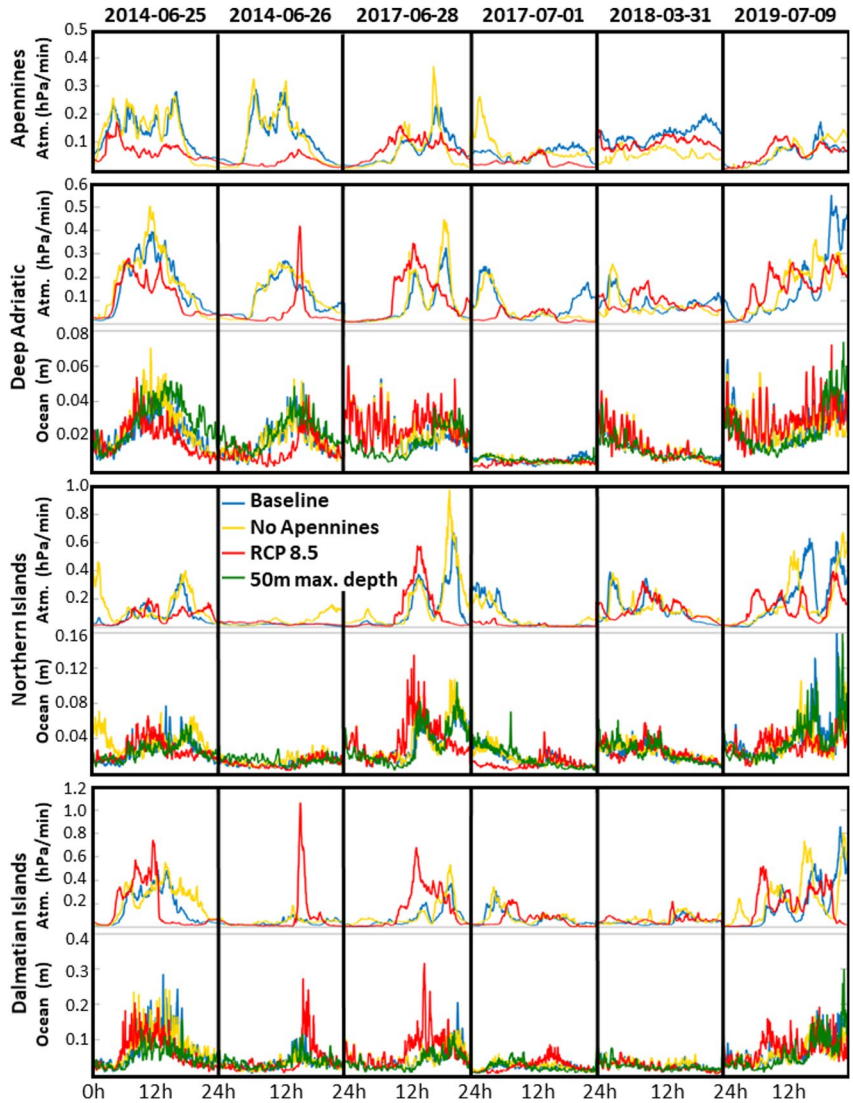

Figure 6. Evolution of the atmospheric disturbance and meteotsunami wave extremes for the four sub-domains. Time variations of the air-pressure rate of change (atm.) and filtered sea-level height (ocean) extreme calculated as the 98th percentile for all points of the four sub-domains (*Apennines*, *Deep Adriatic*, *Northern Islands* and *Dalmatian Islands*) at each time of the events for different experiments (*Baseline*, *No Apennines*, *RCP 8.5* and *50m maximum depth*) and the six studied events.

3.4. Spectral Analysis

Because meteotsunami amplification depends on the local geomorphology, the impacts of orography, bathymetry and climate change to meteotsunami waves are assessed with wavelet and wavelet coherence analyses in the time-period space. The filtered mean sea-level heights are analyzed at three sensitive locations (Figure 1) during three well-reproduced events: in Stari Grad for the 25 June 2014 event, in Vela Luka for the 28 June 2017 event and in Vrboska for the 9 July 2019 event.

Importantly for the meteotsunami propagation, each harbor location has its own amplification factor and resonance frequency. From the time series and the wavelet analyses presented in Figure 7 for the *Baseline* experiment, it can be seen that Vela Luka has the strongest amplification with meteotsunami waves reaching up to 0.80 m of height for periods of 8 and 17 min for one main peak. The amplifications in Stari Grad and Vrboska are lower reaching up to 0.35 and 0.50 m of height for periods of 27 min for two main peaks and 12–15 min for three main peaks, respectively. The time series within the harbors confirm the previous results and show that the

meteotsunami waves decrease at all locations for the *50m maximum depth* experiment and increased up to nearly 1.00 m in height in Vela Luka for the *RCP 8.5* experiment. The *No Apennines* maximum filtered sea-level heights seem not to change much compared to the *Baseline* values.

Concerning the wavelet coherence analyses in the time-period space (Figure 7), they reveal several interesting features during the meteotsunami events. For the *No Apennines* experiment, the time series of filtered sea-levels often have low interdependences (i.e., coherence below 0.40) to their *Baseline* counterparts and are in anti-phase. In other words, the arrows pointing to the bottom-left show that the *No Apennines* meteotsunami events occur after the *Baseline* events for all the periods between 8 and 27 min, with the exception of the first peaks in Stari Grad and Vrboska. For the *RCP 8.5* experiment, the time series generally have high interdependence (coherence above 0.75) but are not in phase. For the second peak only, meteotsunami events occur after their *Baseline* counterparts in Stari Grad and Vrboska but before in Vela Luka. Finally, for the *50m maximum depth* experiment, the time series always have high interdependence (i.e., coherence above 0.75) but are not in phase, with all events occurring after their *Baseline* counterparts.

The spectral analysis thus reveals that environmental changes are impacting not only the intensity of the events but also their timing and, more generally, their behavior in the time-period space.

4. Discussions and Conclusion

In the last century, breakthroughs in computational science and better access to powerful numerical resources have allowed the research community to perform more and more detailed geoscientific studies such as, for example, the impact of climate change on the atmosphere-ocean dynamics (Giorgi, 2019). Recently, in the meteotsunami community, kilometer to sub-kilometer scale coupled atmosphere-ocean modeling suites capable to reproduce the internal atmospheric gravity waves that trigger the meteotsunami events were implemented. These new developments provide the appropriate tools to quantify the influence of different factors (e.g., orography, bathymetry, climate change) on the meteotsunami genesis, thus breaking the barriers of the theoretical, experimental and observational studies. In this work we presented the first results of such a numerical approach.

Our main findings are summarized in Figure 8, presenting the peaks in time (as seen in Figure 6) of both meteotsunami wave and pressure disturbance extremes for each event over each sub-domain (except for the *Apennines* sub-domain which does not cover the Adriatic Sea). They show that:

1. meteotsunami-favorable conditions are likely to be largely increased within the *Dalmatian Islands* sub-domain in both atmosphere and ocean under a projected extreme warming climate (*RCP 8.5* experiment). This is particularly relevant as the strongest and most destructive meteotsunami events occur within this sub-domain (Denamiel et al., 2018, Denamiel, Huan, et al., 2020; Vilibić et al., 2016),
2. however, meteotsunami waves are projected to decrease in the adjacent *Northern Islands* sub-domain under warmer climate (the *RCP 8.5* experiment). Therefore, meteotsunami-favorable conditions are geographically limited due to, for example, the regional bathymetries (flat bathymetry off the *Northern Islands* sub-domain vs. complex and changing bathymetry off the *Dalmatian Islands* sub-domain) or the location of the pressure disturbances during the studied events,
3. flattening of the bathymetry (the *50m maximum depth* experiment) substantially decreases the meteotsunami waves in the *Dalmatian Islands* sub-domain. This indicates that no Proudman resonance occurs within the *Deep Adriatic* sub-domain where the bathymetry is flat. In other words, the speed of atmospheric disturbances is presumably not matching the speed of the long ocean waves in this sub-domain (i.e., 22 m/s). In addition, the flattening is found to divert the meteotsunami waves from the hot-spot locations to neighboring coastal regions. Indeed, changing bathymetry may channelize the meteotsunami energy to certain locations (Šepić et al., 2018; Sheremet et al., 2016), similarly to tsunami propagation over ridges and channels (Titov et al., 2005),
4. removing the Apennines (the *No Apennine* experiment) does not substantially change the intensity of the meteotsunamigenic disturbances (except an increase within the *Apennines* sub-domain) but results in different spatial patterns, particularly for the *Calm Weather* situations. In the ocean, the resulting meteotsunami waves are slightly stronger, presumably due to different characteristic of the meteotsunamigenic disturbances (e.g., speed or propagation direction). Therefore, the meteotsunamigenic disturbances are not generated by the orography, just being modulated, while their origin is presumably driven by shear instabilities or similar processes

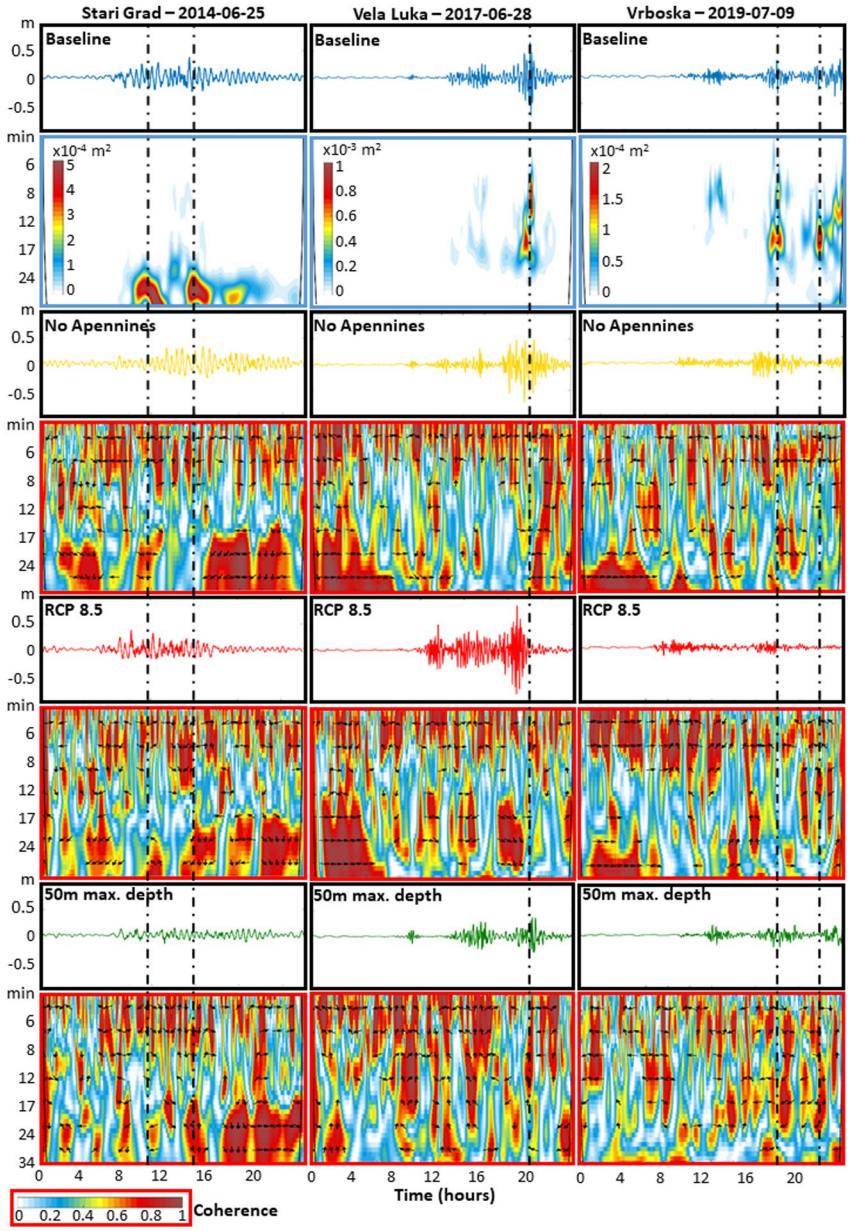

Figure 7. Spectral analysis of the meteotsunami waves in different experiments at sensitive harbor locations. Filtered mean sea-level height time-series (black frames), normalized wavelet power spectrum for the *Baseline* experiment (blue frames) and wavelet coherence for the *No Apennines*, *RCP 8.5* and *50m maximum depth* experiments (red frames) at three sensitive harbor locations along the *Dalmatian Islands* sub-domain for chosen events (Stari Grad for the 25 June 2014 event, Vela Luka for the 28 June 2017 event and Vrboska for the 9 July 2019 event).

that normally generate atmospheric internal gravity waves (Plougonven & Zhang, 2014). That may apply for other world locations vulnerable to meteotsunami events (e.g., the Balearic Islands) for which mountains are also suspected to have a substantial role in the meteotsunami genesis (Jansá & Ramis, 2021).

In terms of physical processes, the findings of this study reveal several interesting mechanisms. First, for all experiments, except for the 9 July 2019 event, the atmospheric disturbances generate meteotsunami waves near the Italian coast. The energy transfers between the atmosphere and the ocean are thus neither pure Proudman resonance (as the bathymetry near the Italian coast is not flat) nor pure Greenspan resonance (as the atmospheric disturbances travel across the Adriatic Sea and not alongshore the Italian coast). Consequently, the energy transfer

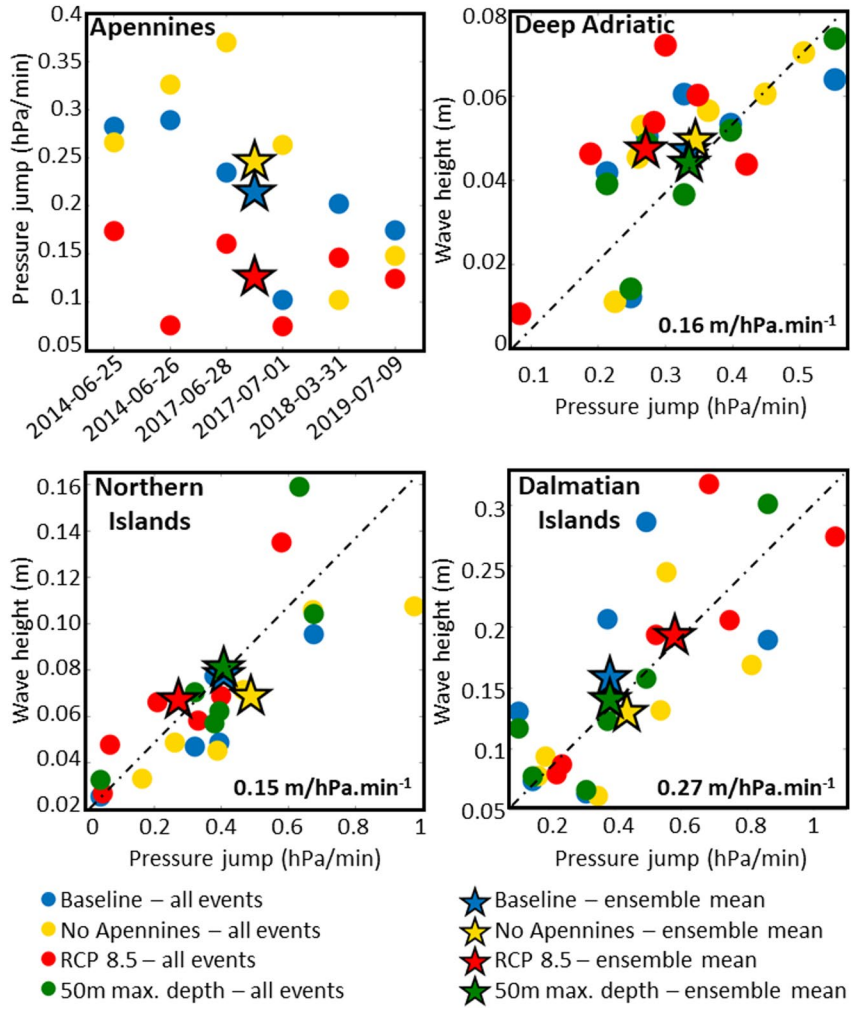

Figure 8. Summary of the findings. For the *Baseline*, *No Apennines* and *RCP 8.5* experiments, peak of the time variations of the 98th percentile for the mean sea-level pressure jump in the atmosphere (as presented in Figure 6) depending on the six selected events for the *Apennines* sub-domain (top left panel). For the four different experiments and all the selected events, peak of the time variations of the 98th percentile for the filtered mean sea-level height (i.e., meteotsunami wave height in the ocean, as presented in Figure 6) depending on the peak of the time variations of the 98th percentile for the air-pressure rate of change in the atmosphere (as presented in Figure 6) for the *Deep Adriatic*, *Northern Islands* and *Dalmatian Islands* sub-domains. For these sub-domains, the linear relationship between the atmospheric disturbance jump and the meteotsunami wave height is given as m/hPa for all events and experiments.

mechanisms along the Italian coast are more complex than the known theories and should be investigated. Second, for the experiment flattening the Adriatic Sea bathymetry at 50 m depth while keeping the shallowest areas untouched (in other word the water depth is given by $H \leq 50m$), all the observed processes can be easily explained with the shallow-water wave propagation and transformation theories. Indeed, the wave-length of all the generated meteotsunami waves L are largely above one km and the shallow-water condition $H/L \leq 0.04$ is always true. Consequently, the meteotsunami waves are strongly affected by the sea bed over the entire Adriatic basin. Hence, shoaling, refraction, reflection and diffraction should be the main processes affecting the propagation of these ocean waves. In fact, our results show that refraction which tends to spread the wave rays over a larger region (here the large area of the middle Adriatic Sea at 50 m depth) is probably the principal transformation process. The meteotsunami waves propagating within the *Deep Adriatic* sub-domain are thus mostly deflected away from the shallower areas of the Adriatic Sea where the shoaling is the strongest. Hence, the large decrease in intensity of the meteotsunami waves within the *Dalmatian Islands* and *Northern Islands* sub-domains observed for most of the events and, of course, the large increase (in percentage) seen within the *Deep Adriatic* sub-domain. Third, concerning the influence of the Apennines, Vilibić and Šepić (2009) hypothesized that the strong fronts present

during meteotsunami events, may be generated or additionally boosted by the orography of the mountains. However, in our study we demonstrated that the Apennines have little impact on the generation of the atmospheric disturbances that trigger meteotsunami events. In fact, compared to the *Baseline* experiment, the intensity of the atmospheric disturbances of the *No Apennines* experiment tends to be increased within the *Apennines* and *Deep Adriatic* sub-domains. Consequently, in the Adriatic Sea, the atmospheric waves observed and modeled during meteotsunami events are not mountain-generated or topographic gravity waves and further research should be carried out to better understand the generation mechanisms of these atmospheric waves. Finally, in terms of the future climate warming influence, one previous study used proxy-derived meteotsunami indices defined at the synoptic scale in the Balearic Islands under RCP 8.5 conditions (Vilibić et al., 2018). Following this work, the number of meteotsunami events at this location is expected to increase by 34% under extreme warming. Yet, contrarily to the approach used in our study, the synoptic meteotsunami index cannot be used to forecast the intensity of these extreme events (Šepić, Vilibić & Monserrat, 2016). Indeed, our results reveal an interesting impact of extreme climate warming on the atmospheric disturbance intensity: It decreases within the *Apennines* sub-domain and increases once the atmospheric waves reach the sea (*Deep Adriatic* sub-domain) but particularly within the *Northern Islands* and *Dalmatian Islands* sub-domains. These findings suggest that, during meteotsunami events, both air-sea and land-sea interactions play a crucial role in the gravity wave dynamics under RCP 8.5 warming conditions. As previously highlighted, more research should be carried out to better understand the propagation and transformation mechanisms of these atmospheric gravity waves.

Notwithstanding the undeniable interest of this study for the meteotsunami community, our analyses present several critical aspects and our conclusions should not be generalized without caution. First, meteotsunami generation and propagation highly depend on the studied geographic location and our results may not be valid outside of the Adriatic basin. Then, the ensemble of six events used in this study is not only small but also includes two meteotsunamis that were not properly reproduced with the AdriSC model (Denamiel, Šepić, Ivanković & Vilibić, 2019). Finally, the found process-level impacts are highly variable from event-to-event depending on the intensity, location and type (i.e., the *Calm Weather* and *Stormy Weather* events) of the meteotsunami conditions. Consequently, we foresee several avenues that can be pursued in future studies to increase the confidence on the presented numerical results. First, the number of events in the studied ensembles should be increased – for example the full catalog of historical meteotsunami events in the Adriatic Sea (Orlić, 2015) should be numerically reproduced. Second, the physics and resolutions of the numerical models should be continuously improved to better capture the coupled atmosphere-ocean meteotsunami dynamics. Then, other geographic locations in the world should be researched – for example, the Balearic Islands (Jansá & Ramis, 2021), the Korean and Japanese west coasts (Choi et al., 2014; Hibiya & Kajiura, 1982), the U.S. East Coast (Churchill et al., 1995; Wertman et al., 2014). Finally, the atmospheric research should be scaled-up within the meteotsunami community which is mostly composed of oceanographers – for example in the Adriatic, only few studies have been led by atmospheric scientists (Belušić et al., 2007; Horvath et al., 2018).

To conclude, we expect that with the constant technological evolutions, sub-kilometer scale coupled atmosphere-ocean models better adjusted to represent meteotsunami events may, in a near future, run at reduced computational cost and allow for radical discoveries concerning the still unknown physics of the meteotsunami generation and propagation.

Acknowledgments
Acknowledgments are made for the support of the European Centre for Middle-range Weather Forecast (ECMWF) staff as well as for ECMWF's computing and archive facilities used in this research. The authors would also like to thank the Editor Robert Hetland, the reviewer Hans Burchard and another anonymous reviewer for their valuable contributions to this article. This work has been supported by projects ADIOS and BivACME (Croatian Science Foundation Grants IP-2016-06-1955 and IP-2019-04-8542, respectively), CHANGE WE CARE (Interreg Italy-Croatia program), and two ECMWF Special Projects ("Using stochastic surrogate methods for advancing towards reliable meteotsunami early warning systems" and "Numerical modelling of the Adriatic-Ionian decadal and inter-annual oscillations: From realistic to process-oriented simulations").

Data Availability Statement

The model results used to produce this article can be obtained under the Open Science Framework (OSF) FAIR data repositories Denamiel (2021a) and Denamiel (2021b).

References

Anderson, E. J., & Mann, G. E. (2021). A high-amplitude atmospheric inertia–gravity wave-induced meteotsunami in Lake Michigan. *Natural Hazards*, *106*, 1489–1501. https://doi.org/10.1007/s11069-020-04195-2

Ban, N., Schmidli, J., & Schär, C. (2015). Heavy precipitation in a changing climate: Does short-term summer precipitation increase faster? *Geophysical Research Letters*, *42*, 1165–1172. https://doi.org/10.1002/2014GL062588

Bechle, A., & Wu, C. (2014). The Lake Michigan meteotsunamis of 1954 revisited. *Natural Hazards*, *74*, 155–177. https://doi.org/10.1007/s11069-014-1193-5

Belušić, D., Grisogono, B., & Klaić, Z. B. (2007). Atmospheric origin of the devastating coupled air-sea event in the east Adriatic. *Journal of Geophysical Research*, *112*, D17111. https://doi.org/10.1029/2006JD008204

Bubalo, M., Janeković, I., & Orlić, M. (2021). Meteotsunami-related flooding and drying: Numerical modeling of four Adriatic events. *Natural Hazards*, *106*, 1365–1382. https://doi.org/10.1007/s11069-020-04444-4

Choi, B.-J., Hwang, C., & Lee, S.-H. (2014). Meteotsunami-tide interactions and high-frequency sea level oscillations in the eastern Yellow Sea. *Journal of Geophysical Research: Oceans*, *119*, 6725–6742. https://doi.org/10.1002/2013JC009788

Churchill, D. D., Houston, S. H., & Bond, N. A. (1995). The Daytona Beach wave of 3–4 july 1992: A shallow water gravity wave forced by a propagating squall line. *Bulletin of the American Meteorological Society*, *76*, 21–32. https://doi.org/10.1175/1520-0477(1995)076<0021:tdbwoj>2.0.co;2

Dee, D. P., Uppala, S. M., Simmons, A. J., Berrisford, P., Poli, P., Kobayashi, S., et al. (2011). The ERA-Interim reanalysis: Configuration and performance of the data assimilation system. *The Quarterly Journal of the Royal Meteorological Society*, *137*, 553–597. https://doi.org/10.1002/qj.828

Denamiel, C. (2021a). *Meteotsunami Genesis - Influence of Environmental Conditions - part1* [Data set]. OSF. https://doi.org/10.17605/OSF.IO/XMEK4

Denamiel, C. (2021b). *Meteotsunami Genesis - Influence of Environmental Conditions - part1* [Data set]. OSF. https://doi.org/10.17605/OSF.IO/WXM7F

Denamiel, C., Huan, X., Šepić, J., & Vilibić, I. (2020). Uncertainty propagation using polynomial chaos expansions for extreme sea level hazard assessment: The case of the eastern Adriatic meteotsunamis. *Journal of Physical Oceanography*, *50*(4), 1005–1021. https://doi.org/10.1175/JPO-D-19-0147.1

Denamiel, C., Pranić, P., Ivanković, D., Tojčić, I., & Vilibić, I. (2021). Performance of the Adriatic Sea and coast (AdriSC) climate component – A COAWST V3.3-based coupled atmosphere–ocean modelling suite: Atmospheric dataset. *Geoscientific Model Development*, *14*, 3995–4017. https://doi.org/10.5194/gmd-14-3995-2021

Denamiel, C., Pranić, P., Quentin, F., Mihanović, H., & Vilibić, I. (2020). Pseudo-global warming projections of extreme wave storms in complex coastal regions: The case of the Adriatic Sea. *Climate Dynamics*, *55*, 2483–2509. https://doi.org/10.1007/s00382-020-05397-x

Denamiel, C., Šepić, J., Huan, X., Bolzer, C., & Vilibić, I. (2019). Stochastic surrogate model for meteotsunami early warning system in the eastern Adriatic Sea. *J. Geophys. Res. Oceans*, *124*, 8485–8499. https://doi.org/10.1029/2019JC015574

Denamiel, C., Šepić, J., Ivanković, D., & Vilibić, I. (2019). The Adriatic Sea and Coast modelling suite: Evaluation of the meteotsunami forecast component. *Ocean Modelling*, *135*, 71–93. https://doi.org/10.1016/j.ocemod.2019.02.003

Denamiel, C., Šepić, J., & Vilibić, I. (2018). Impact of geomorphological changes to harbor resonance during meteotsunamis: The Vela Luka Bay test case. *Pure and Applied Geophysics*, *175*(11), 3839–3859. https://doi.org/10.1007/s00024-018-1862-5

Denamiel, C., Tojčić, I., & Vilibić, I. (2020). Far future climate (2060–2100) of the northern Adriatic air–sea heat transfers associated with extreme bora events. *Climate Dynamics*, *55*, 3043–3066. https://doi.org/10.1007/s00382-020-05435-8

Denamiel, C., Tojčić, I., & Vilibić, I. (2021). Balancing accuracy and efficiency of atmospheric models in the northern Adriatic during severe bora events. *Journal of Geophysical Research: Atmospheres*, *126*, e2020JD033516. https://doi.org/10.1029/2020JD033516

Giorgi, F. (2019). Thirty years of regional climate modeling: Where are we and where are we going next? *Journal of Geophysical Research: Atmospheres*, *124*, 5696–5723. https://doi.org/10.1029/2018JD030094

Greenspan, H. P. (1956). The generation of edge waves by moving pressure distributions. *Journal of Fluid Mechanics*, *1*, 574–592. https://doi.org/10.1017/S002211205600038X

Grinsted, A., Moore, J. C., & Jevrejeva, S. (2010). Application of the cross wavelet transform and wavelet coherence to geophysical time series. *Nonlinear Processes in Geophysics*, *11*, 561–566

Hibiya, T., & Kajiura, K. (1982). Origin of the Abiki phenomenon (a kind of seiche) in Nagasaki Bay. *Journal of the Oceanographical Society of Japan*, *38*, 172–182. https://doi.org/10.1007/bf02110288

Hintze, J. L., & Nelson, R. D. (1998). Violin plots: A box plot-density trace synergism. *The American Statistician*, *52*(2), 181–184. https://doi.org/10.1080/00031305.1998.10480559

Horvath, K., Šepić, J., & Telišman Prtenjak, M. (2018). Atmospheric forcing conducive for the Adriatic: 25 June 2014 meteotsunami event. *Pure and Applied Geophysics*, *175*, 3817–3837. https://doi.org/10.1007/s00024-018-1902-1

Horvath, K., & Vilibić, I. (2014). Atmospheric mesoscale conditions during the Boothbay meteotsunami: A numerical sensitivity study using a high-resolution mesoscale model. *Natural Hazards*, *74*, 55–74. https://doi.org/10.1007/s11069-014-1055-1

Jansá, A., & Ramis, C. (2021). The Balearic rissaga: From pioneering research to present-day knowledge. *Natural Hazards*, *106*, 1269–1297. https://doi.org/10.1007/s11069-020-04221-3

Knupp, K. (2006). Observational analysis of a gust front to bore to solitary wave transition within an evolving nocturnal boundary layer. *Journal of the Atmospheric Sciences*, *63*(8), 2016–2035. https://doi.org/10.1175/jas3731.1

Lanczos, C. (1956). *Applied analysis*. Prentice Hall.

Lindzen, R. (1974). Wave-CISK in the tropics. *Journal of the Atmospheric Sciences*, *31*, 156–179. https://doi.org/10.1175/1520-0469(1974)031<0156:wcitt>2.0.co;2

Lindzen, R. S., & Tung, K. (1976). Banded convective activity and ducted gravity waves. *Monthly Weather Review*, *104*(12), 16022–21617. https://doi.org/10.1175/1520-0493(1976)104<1602:bcaadg>2.0.co;2

Luettich, R. A., Birkhahn, R. H., & Westerink, J. J. (1991). *Application of ADCIRC-2DDI to masonboro inlet*. A brief numerical modeling study Contractors report to the US Army Engineer Waterways experiment station.

Monserrat, S., Rabinovich, A. B., & Casas, B. (1998). On the reconstruction of the transfer function for atmospherically generated seiches. *Geophysical Research Letters*, *25*(12), 2197–2200. https://doi.org/10.1029/98gl01506

Monserrat, S., & Thorpe, A. J. (1996). Use of ducting theory in an observed case of gravity waves. *Journal of the Atmospheric Sciences*, *53*(12), 17242–21736. https://doi.org/10.1175/1520-0469(1996)053<1724:uodtia>2.0.co;2

Monserrat, S., Vilibić, I., & Rabinovich, A. B. (2006). Meteotsunamis: Atmospherically induced destructive ocean waves in the tsunami frequency band. *Natural Hazards and Earth System Sciences*, *6*, 1035–1051. https://doi.org/10.5194/nhess-6-1035-2006

Mourre, B., Santana, A., Builes, A., Gautreau, L., Ličer, M., Jansà, A., et al. (2021). On the potential of ensemble forecasting for the prediction of meteotsunamis in the Balearic Islands: Sensitivity to atmospheric model parameterizations. *Natural Hazards*, *106*, 1315–1336. https://doi.org/10.1007/s11069-020-03908-x

Orlić, M. (2015). The first attempt at cataloguing tsunami-like waves of meteorological origin in Croatian coastal waters. *Acta Adriatica*, *56*, 83–95.

Orlić, M., Belušić, D., Janeković, I., & Pasarić, M. (2010). Fresh evidence relating the great Adriatic surge of 21 June 1978 to mesoscale atmospheric forcing. *Journalof Geophysical Research: Oceans*, *115*, C06011. https://doi.org/10.1029/2009JC005777

Pinardi, N., Allen, I., Demirov, E., De Mey, P., Korres, G., Lascaratos, A., et al. (2003). The Mediterranean ocean forecasting system: First phase of implementation (1998–2001). *Annales Geophysicae*, *21*, 3–20. https://doi.org/10.5194/angeo-21-3-2003

Plougonven, R., & Zhang, F. (2014). Internal gravity waves from atmospheric jets and fronts. *Reviews of Geophysics*, *52*, 33–76. https://doi.org/10.1002/2012RG000419

Powers, J. (1997). Numerical model simulation of a mesoscale gravity-wave event: Sensitivity tests and spectral analyses. *Monthly Weather Review*, *125*, 1838–1869. https://doi.org/10.1175/1520-0493(1997)125<1838:nmsoam>2.0.co;2

Pranić, P., Denamiel, C., & Vilibić, I. (2021). Performance of the Adriatic Sea and coast (AdriSC) climate component—A COAWST V3.3-based one-way coupled atmosphere–ocean modelling suite: Ocean results. *Geoscientific Model Development*, *14*, 5927–5955. https://doi.org/10.5194/gmd-14-5927-2021

Proudman, J. (1929). The effects on the sea of changes in atmospheric pressure. *Geophysical Supplements to the Monthly Notices of the Royal Astronomical Society*, *2*(4), 197–209. https://doi.org/10.1111/j.1365-246x.1929.tb05408.x

Rabinovich, A. B. (2009). Seiches and harbor oscillations. In Y. C. Kim (Ed.), *Handbook of coastal and Ocean engineering* (pp. 193–236). World Scientific Publ. https://doi.org/10.1142/9789812819307_0009

Rabinovich, A. B. (2020). Twenty-seven years of progress in the science of meteorological tsunamis following the 1992 Daytona Beach event. *Pure and Applied Geophysics*, *177*, 1193–1230. https://doi.org/10.1007/s00024-019-02349-3

Rabinovich, A. B., Šepić, J., & Thomson, R. E. (2021). The meteorological tsunami of 1 November 2010 in the southern strait of Georgia: A case study. *Natural Hazards*, *106*, 1503–1544. https://doi.org/10.1007/s11069-020-04203-5

Ramis, C., & Jansà, A. (1983). Condiciones meteorológicas simultáneas a la aparición de oscilaciones del nivel del mar de amplitud extraordinaria en el Mediterráneo Occidental (in Spanish). *Revista Geofísica*, *39*, 35–42.

Renault, L., Vizoso, G., Jansà, A., Wilkin, J., & Tintoré, J. (2011). Toward the predictability of meteotsunamis in the Balearic Sea using regional nested atmosphere and ocean models. *Geophysical Research Letters*, *38*, L10601. https://doi.org/10.1029/2011gl047361

Šepić, J., Međugorac, I., Janeković, I., Dunić, N., & Vilibić, I. (2016). Multi-meteotsunami event in the Adriatic Sea generated by atmospheric disturbances of 25–26 June 2014. *Pure and Applied Geophysics*, *173*, 4117–4138.

Šepić, J., Rabinovich, A. B., & Sytov, V. N. (2018). Odessa tsunami of 27 June 2014: Observations and numerical modelling. *Pure and Applied Geophysics*, *175*, 1545–1572. https://doi.org/10.1007/s00024-017-1729-1

Šepić, J., Vilibić, I., & Monserrat, S. (2016). Quantifying the probability of meteotsunami occurrence from synoptic atmospheric patterns. *Geophysical Research Letters*, *43*, 10377–10410. https://doi.org/10.1002/2016GL070754

Shchepetkin, A. F., & McWilliams, J. C. (2005). The regional oceanic modeling system: A split-explicit, free-surface, topography-following-coordinate Ocean Model. *Ocean Modelling*, *9*(4), 347–404. https://doi.org/10.1016/j.ocemod.2004.08.002

Shchepetkin, A. F., & McWilliams, J. C. (2009). Correction and commentary for "Ocean forecasting in terrain-following coordinates: Formulation and skill assessment of the regional ocean modeling system" by Haidvogel et al. *Journal of Computational Physics*, *227*(24), 3595–3624. https://doi.org/10.1016/j.jcp.2009.09.002

Sheremet, A., Gravois, U., & Shrira, V. (2016). Observations of meteotsunami on the Louisiana shelf: A lone soliton with a soliton pack. *Natural Hazards*, *84*, 471–492. https://doi.org/10.1007/s11069-016-2446-2

Shi, L., Olabarrieta, M., Nolan, D. S., & Warner, J. C. (2020). Tropical cyclone rainbands can trigger meteotsunamis. *Nature Communications*, *11*, 678. https://doi.org/10.1038/s41467-020-14423-9

Simoncelli, S., Fratianni, C., Pinardi, N., Grandi, A., Drudi, M., Oddo, P., & Dobricic, S. (2019), _Mediterranean Sea Physical Reanalysis (CMEMS MED-Physics)_ (Version 1) [Data set]. Copernicus Monitoring Environment Marine Service (CMEMS). https://doi.org/10.25423/MEDSEA_REANALYSIS_PHYS_006_004

Skamarock, W. C., Klemp, J. B., Dudhia, J., Gill, D. O., Barker, D. M., Wang, W., et al. (2005). A description of the advanced research WRF version 2. In *NCAR technical note NCAR/TN-468+STR*. https://doi.org/10.5065/D6DZ069T

Tanaka, K. (2010). Atmospheric pressure-wave bands around a cold front resulted in a meteotsunami in the East China Sea in February 2009. *Natural Hazards and Earth System Sciences*, *10*, 2599–2610. https://doi.org/10.5194/nhess-10-2599-2010

Titov, V., & Moore, C. (2021). Meteotsunami model forecast: Can coastal hazard be quantified in real time? *Natural Hazards*, *106*, 1545–1561. https://doi.org/10.1007/s11069-020-04450-6

Titov, V., Rabinovich, A. B., Mofjeld, H. O., Thomson, R. E., & González, F. I. (2005). The global reach of the 26 December 2004 Sumatra Tsunami. *Science*, *309*(5743), 2045–2048. https://doi.org/10.1126/science.1114576

Tojčić, I., Denamiel, C., & Vilibić, I. (2021). Performance of the Adriatic early warning system during the multi-meteotsunami event of 11–19 May 2020: An assessment using energy banners. *Natural Hazards and Earth System Sciences*, *21*, 2427–2446. https://doi.org/10.5194/nhess-21-2427-2021

Vilibić, I. (2008). Numerical simulations of the Proudman resonance. *Continental Shelf Research*, *28*, 574–581. https://doi.org/10.1016/j.csr.2007.11.005

Vilibić, I., & Šepić, J. (2009). Destructive meteotsunamis along the eastern Adriatic coast: Overview. *Physics and Chemistry of the Earth*, *34*, 904–917.

Vilibić, I., & Šepić, J. (2017). Global mapping of nonseismic sea level oscillations at tsunami timescales. *Scientific Reports*, *7*, 40818. https://doi.org/10.1038/srep40818

Vilibić, I., Šepić, J., Dunić, N., Sevault, F., Monserrat, S., & Jordà, G. (2018). Proxy-based assessment of strength and frequency of meteotsunamis in future climate. *Geophysical Research Letters*, *45*, 10501–10510. https://doi.org/10.1029/2018GL079566

Vilibić, I., Šepić, J., Rabinovich, A. B., & Monserrat, S. (2016). Modern approaches in meteotsunami research and early warning. *Frontiers in Marine Science*, *3*, 57. https://doi.org/10.3389/fmars.2016.00057

Vučetić, T., Vilibić, I., Tinti, S., & Maramai, A. (2009). The Great Adriatic flood of 21 June 1978 revisited: An overview of the reports. *Physics and Chemistry of the Earth*, *34*, 894–903.

Warner, J. C., Armstrong, B., He, R., & Zambon, J. B. (2010). Development of a Coupled Ocean-Atmosphere-Wave-Sediment Transport (COAWST) modeling system. *Ocean Modelling*, *35*, 230–244. https://doi.org/10.1016/j.ocemod.2010.07.010

Wertman, C. A., Yablonsky, R. M., Shen, Y., Merrill, J., Kincaid, C. R., & Pockalny, R. A. (2014). Mesoscale convective system surface pressure anomalies responsible for meteotsunamis along the U.S. East Coast on June 13th, 2013. *Scientific Reports*, *4*, 7143. https://doi.org/10.1038/srep07143

Williams, D. A., Horsburgh, K. J., Schultz, D. M., & Hughes, C. W. (2021). Proudman resonance with tides, bathymetry and variable atmospheric forcings. *Natural Hazards*, *106*, 1169–1194. https://doi.org/10.1007/s11069-020-03896-y